# Optimal Range for Parvalbumin as Relaxing Agent in Adult Cardiac Myocytes: Gene Transfer and Mathematical Modeling

Pierre Coutu* and Joseph M. Metzger[†]

Departments of *Biomedical Engineering and [†]Physiology, University of Michigan, Ann Arbor, Michigan 48109 USA

ABSTRACT   Parvalbumin (PV) has recently been shown to increase the relaxation rate when expressed in intact isolated cardiac myocytes via adenovirus gene transfer. We report here a combined experimental and mathematical modeling approach to determine the dose-response and the sarcomere length (SL) shortening-frequency relationship of PV in adult rat cardiac myocytes in primary culture. The dose-response was obtained experimentally by observing the PV-transduced myocytes at different time points after gene transfer. Calcium transients and unloaded mechanical contractions were measured. The results were as follows. At low estimated [PV] ($\sim$0.01 mM), contractile parameters were unchanged; at intermediate [PV], relaxation rate of the mechanical contraction and the decay rate of the calcium transient increased with little effects on amplitude; and at high [PV] ($\sim$0.1 mM), relaxation rate was further increased, but the amplitudes of the mechanical contraction and the calcium transient were diminished when compared with control myocytes. The SL shortening-frequency relationship exhibited a biphasic response to increasing stimulus frequency in controls (decrease in amplitude and re-lengthening time from 0.2 to 1.0 Hz followed by an increase in these parameters from 2.0 to 4.0 Hz). The effect of PV was to flatten this frequency response. This flattening effect was partly explained by a reduction in the variation in fractional binding of PV to calcium during beats at high frequency. In conclusion, experimental results and mathematical modeling indicate that there is an optimal PV range for which relaxation rate is increased with little effect on contractile amplitude and that PV effectiveness decreases as the stimulus frequency increases.

## INTRODUCTION

Parvalbumin (PV) is an 11-kD protein that belongs to the EF-hand family of calcium ($Ca^{2+}$) binding proteins (Pauls et al., 1996). PV has two metal binding sites, with high affinity for calcium ($K_{pvca} = 10^7–10^9 \ M^{-1}$) and moderate affinity for magnesium ($K_{pvmg} = 10^3–10^5 \ M^{-1}$), with the exact binding constants being species and measurement condition dependent (Pauls et al., 1996). PV is naturally expressed in fast skeletal muscles of vertebrates and in the brain and endocrine glands of mammals (Eberhard and Erne, 1994). In particular, PV's role in fast skeletal muscles has been postulated to involve delayed calcium buffering to increase the relaxation rate (Hou et al., 1992, 1991, West-erblad and Allen, 1994, Rall, 1996, Heizmann et al., 1982). Although PV is not the only requirement for fast relaxation, there is a strong positive correlation between PV concentration and the relaxation rate in mammalian (Heizmann et al., 1982) and frog (Hou et al., 1991) skeletal muscles. In this regard, the toadfish swim bladder muscle is known to be one of the fastest relaxing muscles in the vertebrate world ($t_{1/2R} \cong 5$ ms) (Feher et al., 1998), and it has one of the highest concentrations of PV ([PV] $\cong$ 3 mM) (Rome and Klimov, 2000).

The mechanism for the increase in relaxation rate in fast skeletal muscles due to PV is tightly linked to its delayed (or slow) calcium buffering action (Rall, 1996). The ability of PV to accelerate relaxation in striated muscles can be explained as follows. Under physiological conditions at rest (free [$Mg^{2+}$] $\approx$ 1 mM and [$Ca^{2+}$] $\approx$ 10–100 nM), a large fraction of the PV metal-binding-site population is occupied by magnesium. Upon stimulation, intracellular calcium rises to micromolar levels, causing a fraction of the total divalent binding site population to switch from the magnesium to the calcium-bound state. However, unbinding of magnesium from PV is a relatively slow process ($k_{pvmg}^- = 3.42 \ s^{-1}$ in frog at 20°C (Hou et al., 1992)). This slow unbinding of magnesium from PV causes formation of the PV-$Ca^{2+}$ complex to be delayed when compared with the time course of the rapid transient increase in intracellular free calcium. Due to this delayed action, the amount of calcium buffered during the rapid rising phase of the calcium transient is minimized, whereas after the peak of the calcium transient a significant amount of calcium is buffered. The significant buffering of calcium after the peak of the transient, i.e., during the early decay phase, causes the calcium transient and consequently the mechanical contraction to decay more rapidly. However, at high PV concentrations, it is possible that even the small increase in the fraction of the PV buffering sites occupied by calcium could lead to a depression in the peak amplitude of the calcium transient. To our knowledge, little attention has been paid to this in the literature (Rome et al., 1999).

Although not present endogenously in cardiac muscles, Wahr et al. (1999) have been able to express PV in intact cardiac myocytes via adenovirus gene transfer technology. Using this technique, PV has been successfully expressed at sub-millimolar concentrations in adult rat cardiac myocytes

and has been shown to increase the rate of decay of the calcium transient and the relaxation rate of the mechanically unloaded contraction (Wahr et al., 1999). However, little is known about the quantitative effects of PV concentration on mechanical contraction and calcium transient properties in adult cardiac myocytes.

In this study, we sought to determine the direct effects of PV concentration on the relaxation and contraction properties of membrane intact adult cardiac myocytes in short-term primary culture. We show here the PV dose-response relationship for calcium transients and mechanically unloaded contractions. In particular, attention is placed on the dual effects of PV on the calcium transient: the amplitude attenuation and the acceleration of the decay. We tested the hypothesis that at low PV concentrations there would be no change in mechanical contraction (and/or $Ca^{2+}$ transient) properties, whereas high PV concentrations would result in highly increased relaxation rates with some degree of attenuation in the amplitude of the contraction (and/or $Ca^{2+}$ transient). However, for a given range of intermediate PV concentrations, we hypothesize an ideal case where the contractile amplitude is not reduced significantly whereas the relaxation rate would be increased. This experimentally derived optimal range for PV effects is of critical importance in the case if PV is to be considered as a possible experimental approach to correct diastolic dysfunction in vivo (Szatkowski et al., 2001). Indeed, in diastolic dysfunction, the slowed decay of the calcium transient at the myocyte level (Morgan, 1991) can initiate maladaptive growth at the organ level that could lead ultimately to development of arrhythmia, heart failure, and possibly sudden death (Spirito et al., 2000). In this case, it would be of great importance to improve relaxation speed without impairing the contractile inotropic properties of the heart.

The second main aim of this study involved the determination of the sarcomere length (SL) shortening-frequency relationship in cardiac myocytes in the presence of PV. The SL shortening-frequency relationship is important to address as the dynamic range of the mammalian heart varies from 0.5 to 10 Hz depending on species (human, ~1 Hz; rat, ~6 Hz; mouse, ~10 Hz). During tetanic stimulation of fast skeletal muscles, PV-$Ca^{2+}$ binding sites become saturated, thus limiting the relaxation enhancement of PV (Hou et al., 1992). We therefore hypothesized that in cardiac myocytes, the hastening effects of PV on relaxation will be diminished as the stimulus rate increases. The final aim of this work involved constructing mathematical models that incorporate the effects of PV in the presence of different calcium conditions to aid in the interpretation of the results obtained.

## METHODS

### Solutions

During the myocyte isolation procedure, Krebs-Hensleit buffer (KHB), KHB+$Ca^{2+}$, KHB+$Ca^{2+}$+BSA, and a digestion enzyme solution (DES)

were the principal solutions used. KHB consisted of 118 mM NaCl, 25 mM HEPES, 11 mM glucose, 4.8 mM KCl, 1.2 mM $KH_2PO_4$, and 1.2 mM $MgSO_4$, and the pH was adjusted to 7.4 with HCl. For the KHB+$Ca^{2+}$, 1.0 mM $CaCl_2$ was added to the KHB solution. Bovine serum albumin (BSA) was added to the KHB+$Ca^{2+}$ (final concentration 2%) to form the KHB+$Ca^{2+}$+BSA solution. DES consisted of KHB mixed with hyaluronidase (Sigma Chemical Co., St. Louis, MO) and collagenase (Worthington type II) (final concentration 0.02% and 0.04%, respectively).

For the myocyte plating and primary culture the following solutions were used: DMEM/PS+FBS (plating), DMEM/PS (quiescent cultured myocytes), and M199+ (electrically stimulated cultured myocytes). DMEM/PS was made of Dulbecco's minimal essential medium (DMEM) stock with 50 U/ml penicillin/streptomycin (P/S) (all from GibcoBRL, Gaithersburg, MD). For the DMEM/PS+FBS version, fetal bovine serum (FBS; from GibcoBRL) was added to DMEM/PS for a final concentration of 5%. Finally, M199+ consisted of Media 199 stock (Sigma) supplemented with 10 mM glutathione, 26.2 mM sodium bicarbonate, 0.02% BSA, and 50 U/ml P/S, and the pH was adjusted to 7.4 with NaOH.

For immunofluorescence (IF) experiments, the blocking solution (IF-BS) was made of 20% normal goat serum (NGS) in PBS whereas the antibody solution (IF-AB) consisted of PBS plus 2% NGS plus 0.5% Triton X-100 (TX-100). For Western blot (WB) experiments, the blocking solution (WB-BS) and the antibody solution (WB-AB) were made of 5% dry milk in Tris-buffered saline. For all PV-related WB experiments, 0.05% of polyoxyethylene-sorbitan monolaurate (Tween-20) was incorporated in the solutions.

### Myocyte isolation and gene transfer

Adult cardiac myocytes were isolated from Sprague-Dawley rats (200–250 g) as described previously (Westfall et al., 1997). The isolated myocytes were then plated on laminin-coated coverslips (density of 20,000 rod-shaped myocytes/coverslip) in DMEM/PS+FBS solution for 2 h. The myocytes were incubated with either DMEM/PS solution (control myocytes) or with DMEM/PS solution mixed with adenovirus (PV or *Lac-Z*-transduced myocytes) for an additional hour (Westfall et al., 1997). An optimal multiplicity of infection of 500 plaque-forming units per myocyte (Wahr et al., 1999) was used for both adenoviruses. The myocytes were cultured for up to 4 days in DMEM/PS media as described in Westfall et al. (1997). All perfusion, digestion, and incubation steps were performed at 37°C.

### Electrical stimulation

The coverslips containing myocytes used for mechanical and calcium experiments were transferred to special stimulating chambers 18 h after gene transfer. The chambers (2.5 cm × 3.5 cm) are made of Plexiglas and contain two platinum electrodes each. The chambers were connected to a custom electrical stimulator and a power amplifier (Crown DC-300A). The stimulator supplied a square-wave pulse of 2.5-ms duration at a frequency of 0.5 Hz. The amplitude of the pulse was adjusted such that ~50% of the myocyte population was contracting (Wahr et al., 1999). The media used was the M199+ solution and was replaced every 12 h.

### Parvalbumin expression

The procedure for immunofluorescence detection has been described previously (Westfall et al., 1997). Briefly, coverslips with plated myocytes were fixed with 3% paraformaldehyde/PBS fixative solution for 30 min, treated in blocking solution (IF-BS) for 30 min, followed by a 90-min exposure to primary antibody Parv-19 (Sigma) mixed with IF-AB solution (dilution of 1:1000). After another 30-min blocking period in IF-BS, the

coverslips were exposed to the secondary antibody (goat anti-mouse IgG-Texas Red from Molecular Probes, Eugene, OR; dilution 1:100 in IF-AB).

Western blot experiments were performed as described previously (Westfall et al., 1997). For each sample, the myocytes from two coverslips were scraped and stored in SDS-polyacrylamide gel electrophoresis buffer at $-20°$C until use. Primary antibodies Parv19 and 5c5 (both from Sigma) were used, respectively, to detect parvalbumin and $\alpha$-actin. Dilution of 1:1000 and 1:50,000 in WB-AB were used for Parv-19 and 5c5, respectively. In both cases, goat anti-mouse antibody conjugated to horseradish peroxidase (Sigma A-9917; dilution 1:1000 in WB-AB) was used as the secondary antibody. The detection was performed using the enhanced chemiluminescence technique. Samples collected from rat superior vastus lateralis (SVL) muscle were used as a positive control. For all PV samples, the level of PV expression was normalized to the level of actin expression. The same normalization was also performed on the positive control (SVL). Finally, the PV/actin ratio of PV-transduced myocytes was normalized to the PV/actin ratio of SVL samples to give the estimated PV concentration in myocytes relative to the PV level in SVL. The estimated PV concentration in myocytes is based on a value of 0.4 mM reported for PV concentration in rat SVL (Green et al., 1984).

## Calcium transients

Coverslips were mounted on a custom microscope stage and were kept at 37°C for all experiments. The myocytes were loaded for 6 min in M199+ solution containing 5 $\mu$M fura-2AM (from Molecular Probes) and 0.01% of Pluronic F-127 (from Molecular Probes). After three washes, the myocytes remained in M199+ solution for the measurements. A 5-min period was allowed for de-esterification. Fluorescence was measured using a microscope-based high-speed ratio fluorescence spectrometer (model M-40 from Photon Technology International, Lawrenceville, NJ). The myocytes were electrically stimulated at a frequency <0.2 Hz, and the fluorescence ratio (340 nm/380 nm) was sampled at 100 Hz. Ten sample traces were collected and averaged for each studied myocyte. Smoothing with immediate adjacent time points was performed to reduce noise level. No attempt was made to convert fluorescence ratio into absolute calcium level. The times from stimulus to peak ($t_{P(Ca)}$), to half decay ($t_{S-1/2D(Ca)}$), and to three-fourths decay ($t_{S-3/4D(Ca)}$) were recorded. Curve fitting using custom-fit functions in software Igor (from WaveMetrics, Tucson, AZ) was performed. The decay portion of the curves (from 10% decay to 800 ms after stimulus) were fitted to single- and double-exponential functions.

## Mechanical measurements

The mechanical measurements used the same stage as in the calcium measurements, and the myocytes were also maintained at 37°C in M199+ solution. A HeNe laser diffraction system was used to directly measure the sarcomere length dynamics. A calibrated projection screen was used to estimate the absolute sarcomere length (at $\pm0.05$ $\mu$m). A linear continuous position detector (model LSC-30D from United Detector Technology, Baltimore, MD) was used to collect the position of the first-order diffraction pattern at a sampling rate of 5 kHz as described in Wahr et al. (1999). For the SL shortening study, myocytes were electrically stimulated at 0.2 Hz, and 10 traces were recorded and averaged per myocyte. For the SL shortening-frequency relationship, the myocytes were submitted to at least 15 beats at each frequency, and 3 of the subsequent beats were recorded and averaged. The frequencies used, in order, were 0.2, 0.5, 1.0, 2.0, and 4.0 Hz. The times from stimulus to peak ($t_P$), from peak to half re-lengthening ($t_{1/2R}$), from stimulus to half re-lengthening ($t_{S-1/2R}$), and from half shortening to half re-lengthening or half-width time ($t_{1/2W}$) were recorded. The shortening traces were normalized with respect to their amplitudes, and their maximal positive and negative time derivatives were also measured ($+dl/dt_{max}$ and $-dl/dt_{max}$).

## Mathematical models

Calcium and magnesium binding to PV was calculated using the following equations:

$$\frac{dPvca}{dt} = k^+_{pvca}[Ca^{++}](1 - Pvca - Pvmg) - k^-_{pvca}Pvca$$

$$(1)$$

$$\frac{dPvmg}{dt} = k^+_{pvmg}[Mg^{++}](1 - Pvca - Pvmg) - k^-_{pvmg}Pvmg,$$

$$(2)$$

in which $Pvca$ and $Pvmg$ are the fraction of the PV population binding sites bound with calcium and magnesium, respectively, and $k^+_{pvca}$, $k^+_{pvmg}$, $k^-_{pvca}$, and $k^-_{pvmg}$ are the on and off rate constants of this reaction.

The affinity values used in this paper were obtained from rat PV data at 35°C (Eberhard and Erne, 1994), and are $0.91 \times 10^8$ M$^{-1}$ and $2.43 \times 10^4$ M$^{-1}$ for calcium and magnesium, respectively. The off rates were extrapolated in temperature from frog PV data (Hou et al., 1992), and are $k^-_{pvca}$ = 4.03 s$^{-1}$ and $k^-_{pvmg}$ = 10.58 s$^{-1}$. The on rates were simply calculated from the affinities and the off rates to give: $k^+_{pvca}$ = $3.66 \times 10^8$ M$^{-1}$ s$^{-1}$ and $k^+_{pvmg}$ = $25.71 \times 10^4$ M$^{-1}$ s$^{-1}$. The magnesium concentration was assumed to be of fixed value at 1.0 mM (Godt and Maughan, 1988).

In this study, three different mathematical models incorporating Eqs. 1 and 2 were used: 1) fixed calcium concentration model, 2) fixed calcium transient model, and 3) fixed calcium release model.

In the fixed calcium concentration model, the free calcium concentration ($[Ca^{2+}]$) is used as the stimulus variable using step functions. In this model, PV levels are assumed to be small, therefore not affecting free calcium or magnesium concentrations. The intent of this model is to obtain insights on the kinetics and steady-state values of the fractional binding of PV ($Pvca$, $Pvmg$, $Pvfree = 1 - Pvca - Pvmg$) under a fixed level of free calcium.

The fixed calcium transient model is similar to the fixed calcium concentration model. Free calcium is still being used as the control variable, but a representative calcium transient function is used instead of step functions. This model is used to evaluate the effect of increasing frequency of stimulus on fractional binding of PV. The equation for the calcium transient (Eq. 3) was derived empirically to obtain a calcium transient that has a time to peak of ~20 ms, an exponential decay with $\tau \approx 40$ ms, and a basal and peak level of calcium of 0.1 and 1.0 $\mu$M, respectively. The term to the 8th power is there to ensure that the calcium transient returns to resting level after 250 ms to minimize inter-beat discontinuities at the highest frequency (4 Hz).

$$[Ca^{++}] = 0.0001 \text{ mM} + \frac{0.0019 \text{ mM}}{1 + (t/210 \text{ ms})^8}$$

$$\cdot \{\exp^{(-t/40 \text{ ms})} - \exp^{(-t/10 \text{ ms})}\} \quad (3)$$

The fixed calcium release model is a simplistic version of the myocyte cytoplasmic environment. The purpose of this model is to evaluate the effect of PV on free cytoplasmic calcium concentration during a transient. The model contains a calcium release subunit, a calcium uptake subunit, and calcium cytoplasmic buffers. The calcium release subunit, which represents mostly the calcium release from the sarcoplasmic reticulum (SR), is represented by the following equation:

$$Jrel = (t/12.0 \text{ ms})\exp(-t/12.0 \text{ ms})0.00487 \text{ mM/ms} \quad (4)$$

This equation was derived empirically to resemble the rat cardiac myocyte calcium transient (based on our data; see, e.g., Fig. 3 $A$) in the presence of calmodulin and troponin. The calcium uptake subunit, which

represents mostly uptake via SR Ca$^{++}$ ATPase, is based on the model by Shannon et al. (2000). The equations can be found in Winslow et al. (1999), where they were used in the context of canine cardiac myocytes. The parameter KSR (the scaling factor for calcium ATPase; see Winslow et al., 1999) was changed from 1.0 to 2.3, and [Ca]$_{NSR}$ (the calcium concentration inside the SR; see Winslow et al., 1999) was fixed at 0.262 mM to make the calcium transient decay more rat-like (based on our data; see, e.g., Fig. 3 *A*). The equations for the endogenous calcium buffers are very similar to Eqs. 1 and 2 and are given, along with their parameters, in Robertson et al. (1981) and Winslow et al. (1999) for calmodulin and troponin respectively. PV buffering Eqs. 1 and 2 were also added to the model. PV concentration was used as a variable from simulation to simulation. The free calcium concentration was then calculated as follows:

$$\frac{d[\text{Ca}^{++}]}{dt} = Jrel - Jup - Jpvca - Jhtrpn - Jltrpn$$

$$- Jcmdn \text{ (mM/ms)}, \qquad (5)$$

where *Jrel* and *Jup* are the release and uptake calcium fluxes, respectively, whereas *Jpvca*, *Jhtrpn*, *Jltrpn*, and *Jcmdn* are the buffering calcium fluxes to PV, troponin C high- and low-affinity binding sites, and calmodulin, respectively (Winslow et al., 1999).

For all models, the resulting set of differential equations was solved using a custom program written in C using the fourth order with adaptive time step Runge-Kutta-Merson algorithm (Gerald and Weathley, 1985). These models were chosen to keep external variables under tight control and focus the attention on the role of PV in cardiac myocyte relaxation.

## Statistical analysis

All statistical analysis was performed using GraphPad Instat software. One-way ANOVA was used to determine whether there were any significant differences among multiple groups of data. When there was a significant difference, a Student-Newman-Keuls multiple comparison test was performed to determine which individual groups were different. Values are presented as means along with their standard error.

## RESULTS

### Parvalbumin expression

Adenovirus gene transfer technology has been shown to provide a highly efficient tool to deliver genes into intact adult cardiac myocytes (Westfall et al., 1997). In the present study, we used recombinant adenovirus (E1A deleted) vectors containing either the human $\alpha$-PV or the *Lac-Z* gene (used as a virus control) with transcription driven by the cytomegalovirus promoter (Wahr et al., 1999). To verify the success of gene transfer, we used two different techniques. First, to evaluate the percentage of rod-shaped cardiac myocytes that have been transduced successfully, we used indirect immunofluorescence techniques. Second, to obtain quantitative values for the level of protein expression, we used Western blot techniques. Results of the immunofluorescence experiment are presented in Fig. 1. Fig. 1, *A* and *B*, were taken from coverslips containing PV-transduced myocytes at days 2 and 4 after gene transfer, respectively. The number of rod-shaped myocytes that were PV positive was greater than 95% on day 2 and greater than 99% on days 3 and 4 ($n > 100$ for each case), indicating a high efficiency

and synchronization of PV expression using adenovirus gene transfer technology.

To obtain a quantitative estimate of PV concentration, Western blot analysis of cardiac myocytes along with rat fast twitch muscle standards was used (Fig. 2). As expected, no PV was detected in non-transduced control cardiac myocytes. PV expression increased as a function of days after gene transfer with PV first detected on day 2.0 after gene transfer ([PV] = 0.014 ± 0.005mM). Levels at day 5 were estimated in three experiments and did not show appreciable difference from day 4, indicating apparent saturation (data not shown). The estimated concentration of PV (day 4) in cardiac myocytes was 47.4 ± 5.2% of the amount of PV naturally expressed in SVL muscle. Assuming a SVL PV concentration of 0.4 mM (Green et al., 1984), this corresponds to an estimated PV concentration of 0.19 ± 0.02 mM in cardiac myocytes.

### Calcium transients

Fura-2AM fluorescence (ratio, 340 nm/380 nm) was measured using single twitch contractions (frequency < 0.2 Hz) in cardiac myocytes. The results are summarized in Table 1. Representative calcium transients for control, *Lac-Z-*, and PV-expressing cardiac myocytes (all on day 3 after gene transfer) are presented in Fig. 3 *A*. PV-expressing cardiac myocytes exhibited hastened early decay when compared with either control or *Lac-Z* myocytes but slower decay toward the end of the transient.

For control cardiac myocytes, the $t_{\text{S-1/2D(Ca)}}$ and the fitted decay time constant ($\tau$) for control myocytes at days 2, 3, and 4 were examined. The result showed no significant differences in calcium transient dynamics; therefore, the control myocytes data from days 2–4 were pooled together. The *Lac-Z*-transduced myocytes from days 2–4 were also pooled together as their calcium transient dynamic parameters were unchanged over that time period. Fig. 3 *B* shows $t_{\text{S-1/2D(Ca)}}$ for the three myocyte groups. The pooled control and *Lac-Z* myocytes exhibited no differences in their $t_{\text{S-1/2D(Ca)}}$, whereas at day 2 the PV-expressing myocytes showed a moderate but statistically significant reduction in $t_{\text{S-1/2D(Ca)}}$ when compared with the control myocytes. This reduction in decay time was more pronounced by days 3 and 4 for PV-expressing myocytes. The $t_{\text{S-3/4D(Ca)}}$ was also determined (Table 1). In this analysis, only day 3 PV-expressing myocytes showed a significant reduction in $t_{\text{S-3/4D(Ca)}}$ when compared with control. This indicates that, in PV-expressing myocytes, the early part of the decay process is accelerated but not the later part. This phenomenon will be addressed in the Discussion.

To more completely assess the calcium transients, the traces were fit with single- and double-exponential functions (results in Table 1). The fit started at 10% of the decay and ended at 800 ms after stimulation. All control and *Lac-Z*-transduced myocytes were well fit by single-expo-
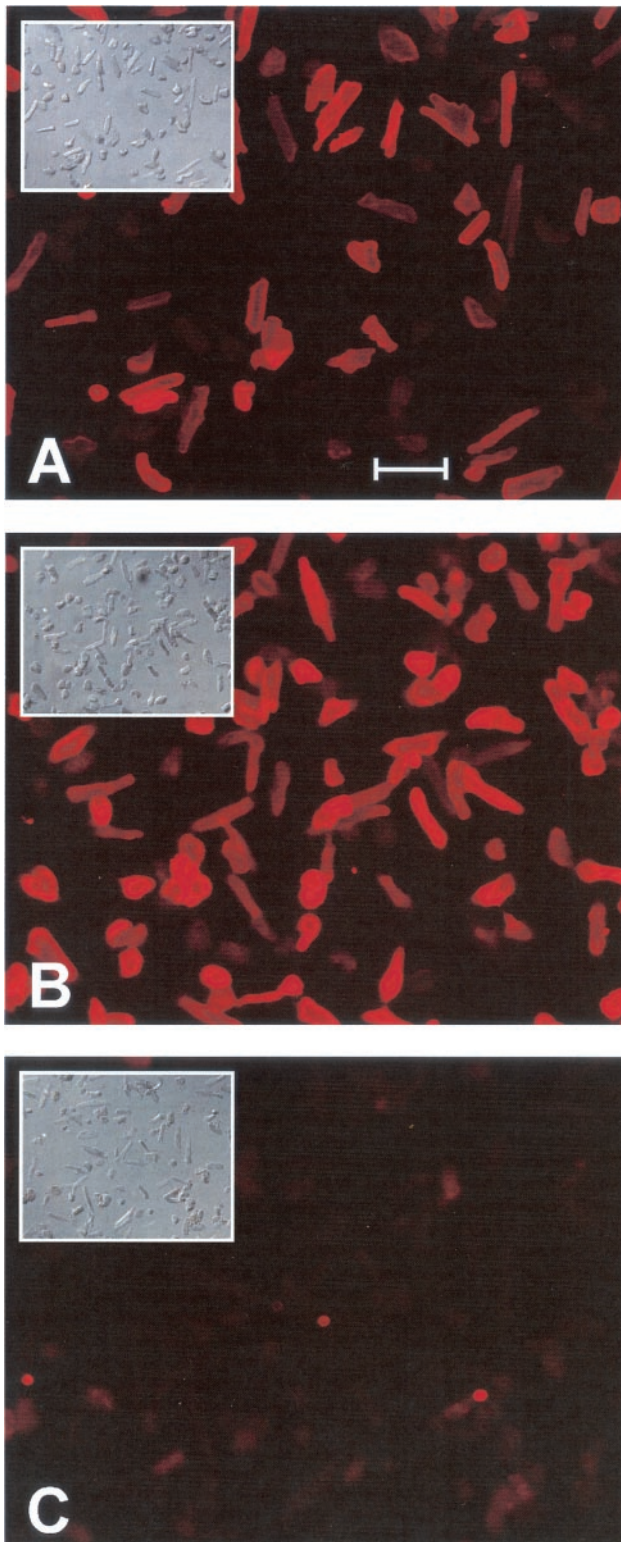
FIGURE 1 Immunofluorescence detection of PV in rat adult cardiac myocytes. (*A*) PV-transduced myocytes on day 2 post gene transfer (PGT); (*B*) PV-transduced myocytes on day 4 PGT; (*C*) Control myocytes on day 4. The main panels show myocytes treated with primary antibody Parv-19 and secondary antibody anti-mouse IgG-Texas Red. Images were taken using fluorescence microscopy. The calibration bar in *A* indicates a length of 100 $\mu$m. The insets show the same myocytes under IDC-bright field illumination.
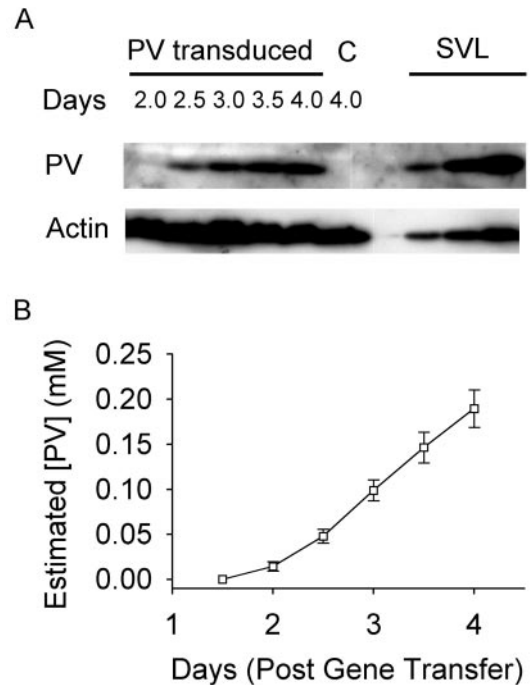


FIGURE 2 Western blot analysis of PV expression at different time points post gene transfer (PGT). (*A*) Representative Western blot. The top row is PV expression, and the bottom row is the actin expression (used for the normalization). As expected, control myocytes (C) show no traces of endogenous PV, whereas PV expression increases as function of days PGT in PV-transduced myocytes. (*B*) Summary of estimated [PV] versus days PGT. The results in myocytes were scaled relative to SVL. The [PV]$_{SVL}$ was assumed to be equal to 0.4 mM (Green et al., 1984). Values are mean with SEM ($n = 10$–16).

nential functions (Fig. 4 *A*). Fitting a double exponential did not visually improve the quality of the fit in most cases. To confirm this visual impression, a $\chi^2$ test was performed on each fit. On average, the $\chi^2$ value was reduced by only 16.5 $\pm$ 2.3% for the control and by 20.9 $\pm$ 2.4% for the *Lac-Z* myocytes. However, for 80% of the PV-transduced myocytes, there was a striking visual improvement by going from the single- to the double-exponential fit (Fig. 4 *B*). Moreover, the $\chi^2$ value was reduced, on average, by 70.0 $\pm$ 2.3%, 62.3 $\pm$ 3.0%, 66.6 $\pm$ 3.2% on days 2, 3, and 4, respectively, for this group. The remaining 20% of the PV population showed only a 17.4 $\pm$ 6.5% reduction in $\chi^2$ value when going from single- to double-exponential fit. The double-exponential fit was rejected if at least one of the following conditions was met: small reduction in $\chi^2$ value ($<$20%), small contribution of the slow component ($<$3%), the slow and fast time constant were identical (within 5%), or the slow time constant was $>$3 SD away from the mean.

In the double-exponential fit of PV-expressing myocytes the slow component contributed 14.6 $\pm$ 1.1%, 11.9 $\pm$ 1.1%, and 13.3 $\pm$ 1.0% of the total amplitude for days 2, 3, and 4, respectively (not significantly different from each other). The slow time constant was 0.954 $\pm$ 0.110 s, 0.898 $\pm$ 0.072

**TABLE 1 Summary of calcium transient and sarcomere shortening measurements**

| | Control (pooled) | *Lac*-Z (pooled) | PV | | | | |
|---|---|---|---|---|---|---|---|
| | | | Day 1 | Day 2 | Day 2.5 | Day 3 | Day 4 |
| Calcium transient | | | | | | | |
| $n$ | 105 | 105 | – | 26 | – | 48 | 49 |
| $t_{P(Ca)}$ (ms) | 49.0 (1.5)* | 49.2 (1.6) | – | 39.2 (1.6) | – | 42.7 (1.8)[†] | 43.9 (2.2)[‡] |
| $t_{S-1/2D(Ca)}$ (ms) | 180.5 (2.5) | 178.4 (2.8) | – | 159.6 (4.4)[§] | – | 142.7 (3.9)[¶] | 143.5 (4.6)[¶] |
| $t_{S-3/4D(Ca)}$ (ms) | 273.1 (4.4) | 275.6 (5.7) | – | 280.2 (11.3) | – | 245.8 (9.5)[‖] | 258.7 (8.3) |
| $n$ (single-exponential fit) | 105 | 105 | – | 4 | – | 11 | 10 |
| $\tau$ (ms) | 151.0 (3.8) | 157.9 (5.0) | – | 124.7 (13.5) | – | 136.9 (8.1) | 129.4 (6.9) |
| $n$ (double-exponential fit) | – | – | – | 22 | – | 37 | 39 |
| $A_{SLOW}$ (%) | – | – | – | 14.6 (1.1) | – | 11.9 (1.1) | 13.3 (1.0) |
| $\tau_{SLOW}$ (ms) | – | – | – | 954 (110) | – | 898 (72) | 1060 (103) |
| $\tau_{FAST}$ (ms) | – | – | – | 114.7 (5.8) | – | 75.4 (3.6) | 78.7 (3.9) |
| Sarcomere shortening | | | | | | | |
| $n$ | 175 | 149 | 54 | 61 | 52 | 63 | 59 |
| Amplitude (nm) | 96.1 (2.1) | 95.0 (2.3) | 99.1 (3.1) | 94.4 (3.3) | 93.5 (4.7) | 82.3 (4.0)[‖] | 73.2 (3.6)[¶] |
| $t_P$ (ms) | 47.4 (0.7) | 47.6 (0.7) | 51.1 (1.2)[§] | 45.8 (1.3) | 41.7 (1.1)[¶] | 37.3 (0.9)[¶] | 37.4 (1.0)[¶] |
| $t_{P-1/2R}$ (ms) | 23.5 (0.6) | 23.9 (0.6) | 23.4 (1.0) | 21.9 (1.2) | 21.0 (1.0) | 19.2 (1.2)[§] | 17.3 (0.9)[¶] |
| $t_{S-1/2R}$ (ms) | 70.9 (1.0) | 71.5 (0.9) | 74.5 (1.6) | 67.7 (1.9) | 62.7 (1.6)[§] | 56.5 (1.7)[¶] | 54.7 (1.5)[¶] |
| $t_{1/2W}$ (ms) | 50.0 (1.0) | 50.4 (0.9) | 53.4 (1.7) | 47.9 (1.8) | 43.8 (1.5)[§] | 38.9 (1.8)[¶] | 35.3 (1.3)[¶] |
| $+dl/dt$ max (1/s) | 54.3 (1.1) | 54.3 (1.1) | 50.5 (1.6) | 54.2 (1.7) | 62.3 (2.6)[¶] | 69.7 (1.8)[¶] | 69.7 (2.2)[¶] |
| $-dl/dt$ max (1/s) | −45.1 (1.3) | −44.0 (1.0) | −44.1 (2.5) | −44.6 (2.1) | −50.3 (2.1) | −54.7 (2.6)[¶] | −59.5 (2.6)[¶] |

Control and Lac-Z measurements taken at different days after gene transfer were pooled into a single group. $t_{P(Ca)}$, $t_{S-1/2D(Ca)}$, and $t_{S-3/4D(Ca)}$ represent the time from stimulus to peak, time from stimulus to half and three-fourths decay of the calcium transients, respectively. $\tau$ represents the time constant for the single-exponential fit, whereas $A_{SLOW}$, $\tau_{SLOW}$, and $\tau_{FAST}$ are the relative contribution of the slow component, the slow time constant, and the fast time constant, respectively, for the double-fitted calcium transient decay. $t_P$, $t_{P-1/2R}$, $t_{S-1/2R}$, $t_{1/2W}$, $+dl/dt$ max, and $-dl/dt$ max are the time to peak, time from peak to half re-lengthening, time from stimulus to half re-lengthening, time of half-width, and the maximal positive and negative time derivatives of normalized sarcomere shortening, respectively. Values are indicated as means with SEMs in parentheses. $n$, number of myocytes per group.

*Control data $T_{P(Ca)}$ showed significant differences between daily values ($41.9 \pm 1.9$ ms, $54.7 \pm 2.4$ ms, and $50.3 \pm 3.0$ ms for days 2, 3, and 4, respectively); the data were pooled only for completeness.

[†][‡]Values significantly different from control data from the corresponding day: [†]$p < 0.001$; [‡]$p < 0.05$.

[§][¶][‖]Values significantly different from pooled control values: [§]$p < 0.01$; [¶]$p < 0.001$; [‖]$p < 0.05$.

s, and $1.060 \pm 0.103$ s on days 2, 3, and 4, respectively (not significantly different from each other). A summary of the fast (or single) time constant values is presented in Fig. 4 *C*. The fast time constant is shown for the 80% of the PV population that was better fit with a double exponential whereas the single time constant is shown for the remaining 20% of the PV myocyte population. Overall, there was a large and significant reduction in the fast time constant, especially on days 3 and 4 for PV-expressing myocytes when compared with the control myocytes. A possible cellular basis for the double-exponential fit for the PV-transduced myocytes will be addressed in the Discussion.

## Mechanical measurements

Using the laser diffraction technique, the kinetics of unloaded sarcomere shortening were measured. A summary of the results is presented in Table 1. Representative data are shown in Fig. 5 *A* for day 3 control, *Lac-Z-*, and PV-expressing myocytes. The $t_{S-1/2R}$ for each myocyte group is summarized in Fig. 5 *B*. In control and *Lac-Z* myocytes, the $t_{S-1/2R}$ was not significantly altered over time in primary

culture. Therefore, for both control and *Lac-Z* groups, data from all days (1.0, 2.0, 3.0, and 4.0) were pooled together. At day 2, PV-expressing myocytes did not show any significant reduction in $t_{S-1/2R}$. However, starting at day 2.5 and increasing through day 4, $t_{S-1/2R}$ for PV-expressing myocytes was significantly shorter, indicating a faster rate of relaxation as a function of increased PV expression (Fig. 2 *B*).

A calibrated screen was used to measure the resting SL and contraction amplitude. The resting SL of individual myocytes ranged from 1.6 to 1.9 $\mu$m, with averages ranging from 1.76 to 1.80 $\mu$m per group. A summary of the effects of PV expression on the amplitude of SL shortening is presented in Fig. 5 *C*. The day 1 to day 4 data were pooled together for control and *Lac-Z* myocytes. The control, *Lac-Z*, and the initial days PV data (days 1.0, 2.0, and 2.5) showed no significant differences in the amplitude of shortening. However, at days 3.0 and 4.0, the contraction amplitude for PV-expressing myocytes was smaller than the control. It should be noted that for PV myocytes on day 2.5, the amplitude of contraction was not significantly altered whereas the $t_{S-1/2R}$ was significantly reduced. This point will become important in determining optimal level of
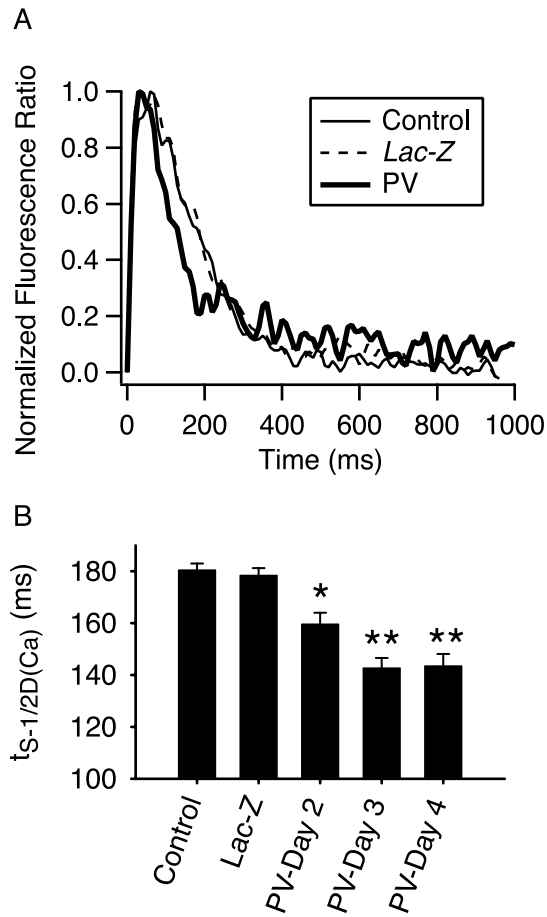
FIGURE 3   Calcium transients. (*A*) Representative calcium transients from single cardiac myocytes (*thick line*, PV; *dashed line*, *Lac-Z*; *thin line*, control; all data are from day 3); (*B*) Summary of the time from stimulus to half-decay of the calcium transient for the three groups. Data from day 2 to 4 for *Lac-Z* and control myocytes were not different and were pooled, whereas data for PV is shown for days 2–4 ($n = 105$ for control and *Lac-Z*; $n = 26$, 48, and 49 for PV days 2, 3, and 4, respectively). Asterisks indicate significant difference from pooled control (*$p < 0.01$, **$p < 0.001$). Values are mean with SEM.

PV for which contraction relaxation is faster but its amplitude is not impaired (see Discussion).

In another set of experiments, the effects of PV expression on SL shortening-frequency relationship was determined. The stimulation frequency was varied from 0.2 to 4 Hz. For each frequency, a minimum of 15 beats was allowed to reach steady state and 3 subsequent sample beats were recorded and averaged. Measurements were made on days 2 and 3. Fig. 6 *A* shows a representative shortening amplitude-frequency response for a control myocyte on day 3. In agreement with previous work in primary culture, the response was biphasic, with a decreasing amplitude response observed between 0.2 and 1.0 Hz (Lim et al., 2000; Hattori et al., 1991; Stemmer and Akera, 1986) and an increasing amplitude response observed from 2.0 to 4.0 Hz (Lim et al., 2000). Control (day 2), *Lac-Z-* (days 2 and 3),
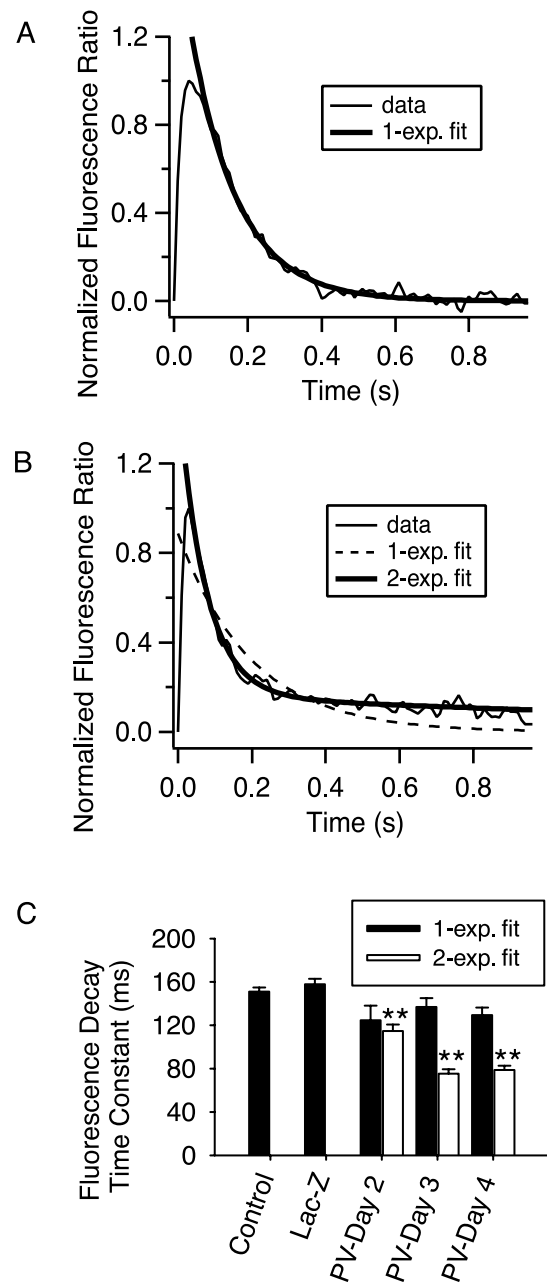


FIGURE 4   Calcium transient curve fitting. (*A*) All control, *Lac-Z*, and 20% of PV myocytes were well fit by single-exponential function; (*B*) The remaining 80% of the PV population required a double-exponential fit; (*C*) Summary of the fast (or single) time constant obtained with the fits. The single time constant for control and *Lac-Z* myocytes showed no significant difference between days after gene transfer and were pooled together. The single and the fast (for the portion of the population that was better fit with a double exponential) time constants are shown as function days after gene transfer for PV-transduced myocytes. Number of samples from left to right are $n = 105$, 105, 4, 22, 11, 37, 10, and 39. Asterisks indicate significant difference from pooled control (**$p < 0.001$). Values are mean with SEM.

and PV-expressing (day 2) myocytes exhibited similar results. However, by day 3 where PV expression is increased (Fig. 2 *B*), the normalized amplitude response for the PV-
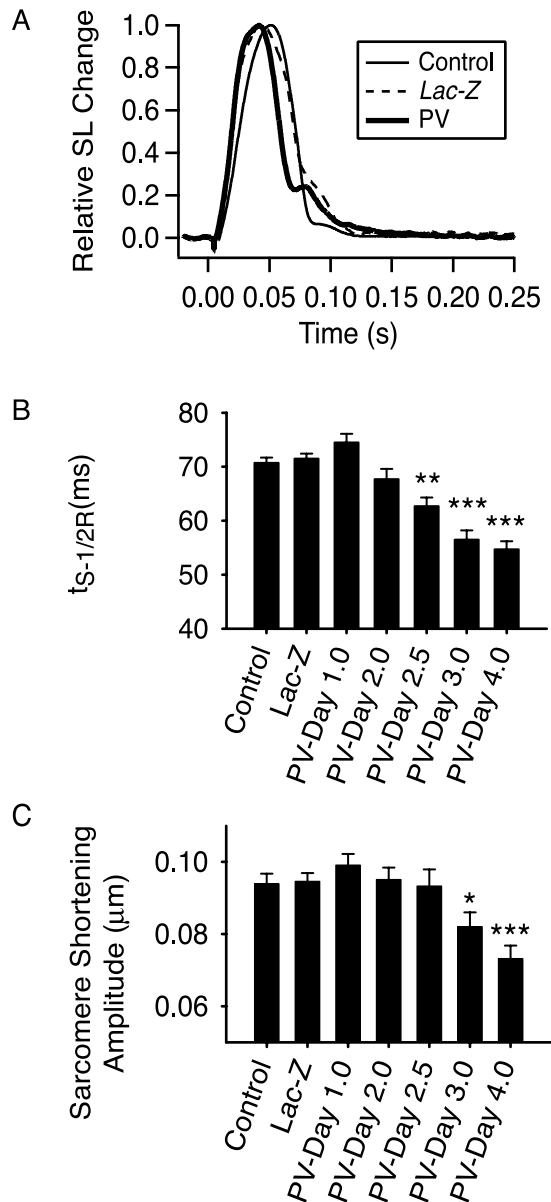
FIGURE 5  Sarcomere shortening data. (A) Representative traces of control, *Lac-Z*, and PV-transduced cardiac myocytes (day 3); (B) Summary of time from stimulus to half re-lengthening; (C) Summary of amplitude of sarcomere shortening. Results for control ($n = 175$; days 1–4 pooled) and *Lac-Z* ($n = 149$; days 1–4 pooled) myocytes and PV ($n = 54, 61, 52, 63$, and 59 for days 1, 2, 2.5, 3, and 4, respectively) are expressed as function of days after gene transfer. Asterisks indicate significant difference from pooled control (*$p < 0.05$; **$p < 0.01$; ***$p < 0.001$). Values are mean with SEM.
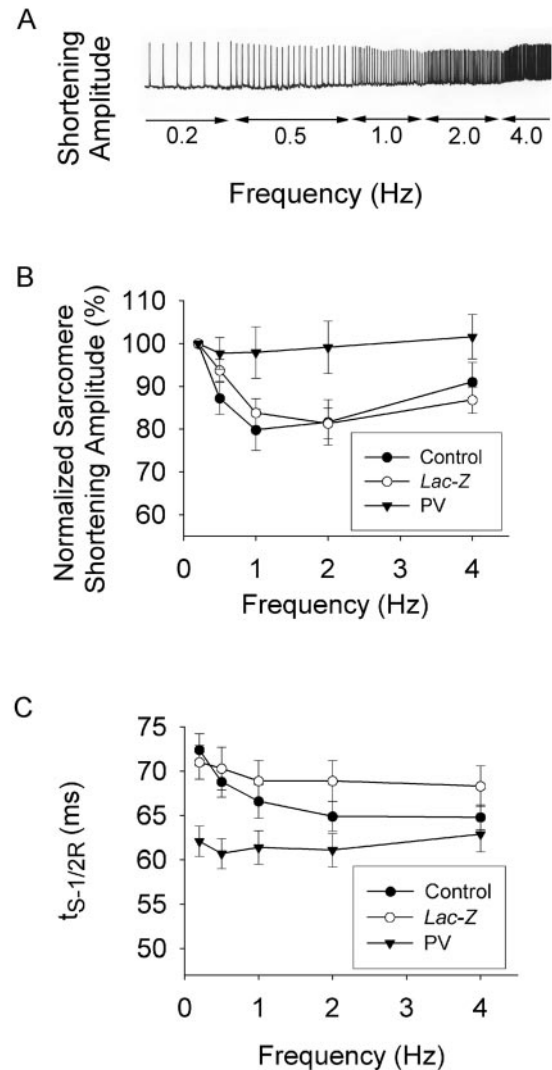


FIGURE 6  Sarcomere length shortening-frequency response. (A) Representative SL shortening-frequency response for a control myocyte. The amplitude of the shortening is displayed as function of time. Stimulus frequencies are indicated. (B) Frequency response of sarcomere shortening amplitude normalized to the 0.2-Hz value. Results are for control, *Lac-Z*, and PV myocytes on day 3. (C) Time from stimulus to half re-lengthening as a function of frequency for control ($n = 25$), *Lac-Z* ($n = 26$), and PV ($n = 25$) myocytes on day 3. Values are mean with SEM.

expressing myocytes was flatter (Fig. 6 *B*). The $t_{S-1/2R}$ is presented in Fig. 6 *C* (day 3). At 0.2 Hz, the PV expressing myocytes showed a more rapid relaxation (as in Fig. 5B). However, as the frequency increased, the $t_{S-1/2R}$ in PV-expressing myocytes did not decrease as it did for *Lac-Z* and control myocytes. Although the nature of the biphasic frequency response of the control cardiac myocytes is still

unknown, a possible basis for the effects of PV on this response is presented in the Discussion.

## Mathematical models

Using mathematical models, we sought to obtain insights into how PV concentration affects the shape and kinetics of the calcium transient. One of the simplest models that could be considered is the fixed calcium concentration model. In this model, PV is submitted to a step function for the calcium, and this value remains constant for the duration of the step. Under these conditions, if the step is long enough,

the fractional binding variables of PV, *Pvca* and *Pvmg*, reach a steady state (ss) value given by the following equations:

$$Pvca_{ss} = \frac{-Apvmg}{1 - (1 + Apvca)(1 + Apvmg)} \qquad (6)$$

$$Pvmg_{ss} = \frac{-Apvca}{1 - (1 + Apvca)(1 + Apvmg)}, \qquad (7)$$

where:

$$Apvca = \frac{k_{pvca}^-}{k_{pvca}^+[Ca^{++}]} \qquad (8)$$

$$Apvmg = \frac{k_{pvmg}^-}{k_{pvmg}^+[Mg^{++}]} \qquad (9)$$

If we take the calcium concentration as a constant for the duration of the step, the system of equations described by Eqs. 1 and 2 becomes a set of coupled ordinary differential equations. By using eigenvalue analysis, it is possible to uncouple the equations and find the time constants required to reach steady state. The time constants are given by:

$$\tau^+ = \frac{2}{(a11 + a22) + \sqrt{(a11 + a22)^2 - 4(a11 \times a22 - a12 \times a21)}} \qquad (10)$$

$$\tau^- = \frac{2}{(a11 + a22) - \sqrt{(a11 + a22)^2 - 4(a11 \times a22 - a12 \times a21)}} \qquad (11)$$

where:

$$a11 = k_{pvca}^+[Ca^{++}] + k_{pvca}^- \qquad (12)$$

$$a12 = k_{pvca}^+[Ca^{++}] \qquad (13)$$

$$a21 = k_{pvmg}^+[Mg^{++}] \qquad (14)$$

$$a22 = k_{pvmg}^+[Mg^{++}] + k_{pvmg}^- \qquad (15)$$

Using the values for the different constants given in Methods, assuming a clamped value of $[Ca^{2+}] = 1.0 \ \mu M$, the steady-state values for fractional binding become $Pvca_{ss} = 0.782$ and $Pvmg_{ss} = 0.209$. The time constants obtained with these values are $\tau^- = 127.2$ ms and $\tau^+ = 1.59$ ms.

A simulation of a calcium clamp using the values mentioned above is presented in Fig. 7 *A*. As seen from the simulation, only a small fraction of the PV population is unbound. When the calcium level rises (inset), there is a small decrease in the PV-free population toward the calcium-bound state. This transition occurs on the order of the fast time constant ($\tau^+$). However, this contribution is of negligible amplitude. Most of the calcium buffering occurs on a much slower time scale ($\tau^-$), and *Pvca* takes its increase mostly via a decrease in the *Pvmg* population, i.e., unbinding of magnesium from PV.

To obtain positive lusitropic effects (acceleration of the decay/relaxation phase) without any reduction in contractile amplitude the two following conditions must be met. 1) At the peak of the calcium transient, the amount of calcium buffered by PV must be small compared with the amount of calcium buffered by troponin, calmodulin, and other endogenous buffers (to avoid a further reduction in amplitude). 2) In the first part of the decaying phase, the amount of calcium buffered by PV should be comparable to the amount of calcium buffered by other buffers (to see a significant increase in relaxation speed). Fig. 7 *B* illustrates that point. A clamp of 150-ms duration at $[Ca^{2+}] = 1 \ \mu M$ was applied to the model (at [PV] = 0.03 mM), and the variation in the amount of calcium buffered by calmodulin and troponin was also computed. At the point where a typical rat calcium transient peak (*Pk*) would be (~30 ms after stimulus), the amount of calcium buffered by PV corresponded to ~15% of the amount absorbed by the other buffers. At the point where one-quarter decay (*Dc*) would occur in rat cardiac myocytes (~120 ms after stimulus) PV buffered 38% of the amount buffered by the other calcium buffers.

In controlling the effectiveness of the delayed calcium buffer action, three parameters are of primary importance: 1) the variation in the fraction of PV sites occupied by calcium during a single beat ($\Delta Pvca$), 2) the time constant at which the binding occurs (mostly dominated by $\tau^-$), and 3) the PV concentration ([PV]). The amount of calcium buffered by PV as a function of time is plotted in Fig. 7 *C* for several different cases where the stimulus is a short pulse-wave calcium clamp (duration 150 ms, frequency 1 Hz). The thick solid line represents the control case where [PV] is 0.02 mM and all the parameters are set as mentioned in Methods. The thin solid line represents the case where PV concentration is halved to 0.01 mM. The thick dashed lined represents the case where the rate constants were $k_{pvca}^- = 2.69 \ s^{-1}$, $k_{pvmg}^- = 4.81 \ s^{-1}$ such that the time constant ($\tau^-$) was doubled. Finally, the thin dashed line represents the
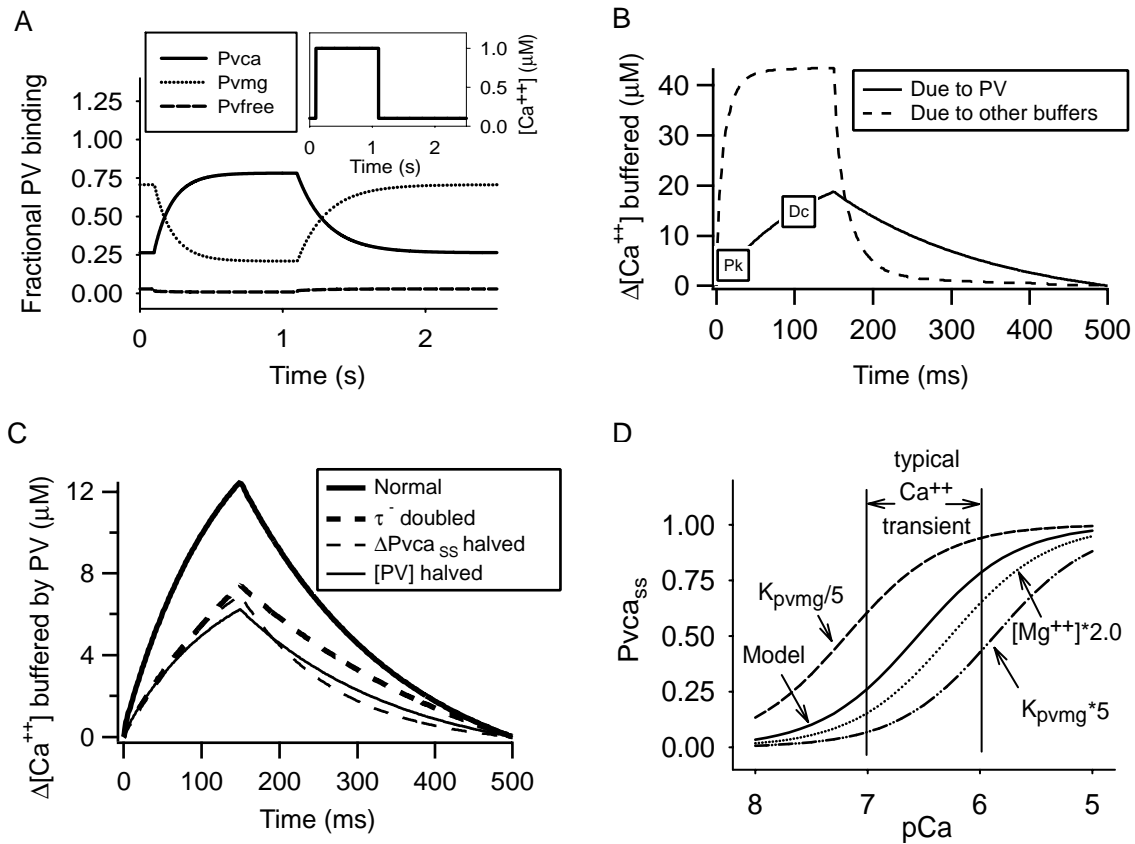
FIGURE 7    Simulation of PV fractional binding to calcium and magnesium (fixed calcium concentration model). (*A*) Simulation of PV fractional binding (main figure) when calcium is stepped from 0.1 to 1.0 $\mu$M (*inset*); (*B*) Buffering capacity of PV. The traces represent the amount of calcium buffered by PV (*solid*) and by troponin and calmodulin (*dashed*) during a short duration calcium clamp (150 ms at 2 Hz). Pk and Dc indicate where the peak and the 25% decay portion of a typical rat cardiac myocyte calcium transient would be. (*C*) Parameters that control calcium buffering by PV. Results show the effects of halving [PV] (*thin solid*), doubling time constant $\tau^-$ (*thick dash*) or halving $\Delta Pvca$ (*thin dashed*) on the amount of calcium buffered by PV during a pulse-wave calcium clamp (as in *B*). The thick solid line represents control case; see text for all details. (*D*) Effects of altered model parameters on $Pvca_{ss}$. The PV-Mg$^{2+}$ affinity constant was divided by 5 (*dashed*) or multiplied by 5 (*dashed-dot*), the magnesium concentration was doubled (*dot*). Results indicate large changes in $Pvca_{ss}$, but the amount of variation in $Pvca_{ss}$ between typical calcium transient diastolic and systolic values remains similar.

case where variation in the fraction of PV site population occupied by calcium during a single beat ($\Delta Pvca$) was halved again by adjusting the PV reaction rate constants ($k_{pvca}^+ = 2.44 \times 10^8$ M$^{-1}$ s$^{-1}$, $k_{pvca}^- = 8.06$ s$^{-1}$, $k_{pvmg}^+ = 5.01 \times 10^5$ M$^{-1}$ s$^{-1}$, $k_{pvmg}^- = 7.30$ s$^{-1}$). Basically, the results show that each of these three parameters can be varied such that they give a similar amount of calcium buffered during a single beat. In the system that we are currently using experimentally, the on and off rates of the PV reaction are fixed leaving PV concentration (e.g., Fig. 2 *B*) as the only variable for a given calcium transient. However, one could envision mutations on the EF-hand motifs of PV, which would modify the other parameters.

To investigate the sensitivity of the models, we examined how changes in the model constants would affect the variation in fractional binding ($\Delta Pvca$). In Fig. 7 *D*, the steady-state value of the fraction of the PV population bound to calcium ($Pvca_{ss}$) is plotted as a function of calcium concentration for four different cases. The vertical lines indicate,

respectively, diastolic ($pCa = 7.0$) and systolic ($pCa = 6.0$) values of a typical calcium transient. The solid curve represents the response obtained with the model values as described in Methods. The important parameter to consider in this response is the variation in $Pvca_{ss}$ between the two vertical lines, which would be proportional to $\Delta Pvca$ for a given calcium transient. If the magnesium concentration is doubled from 1 to 2 mM or if the value of the magnesium affinity was increased or decreased by a factor of 5, the $Pvca_{ss}$ traces would change significantly as seen in Fig. 7 *D*. However, the amount of variation in $Pvca_{ss}$ still remains at similar levels even with large variations in these parameters. This point emphasizes that even though the quantitative values of the models are not exact, the qualitative results obtained should still be significant.

Although the fixed calcium concentration model simulations lend insight into the kinetics and amplitude in the PV-binding population, it is very difficult to measure these variables experimentally. Instead, one must rely on the
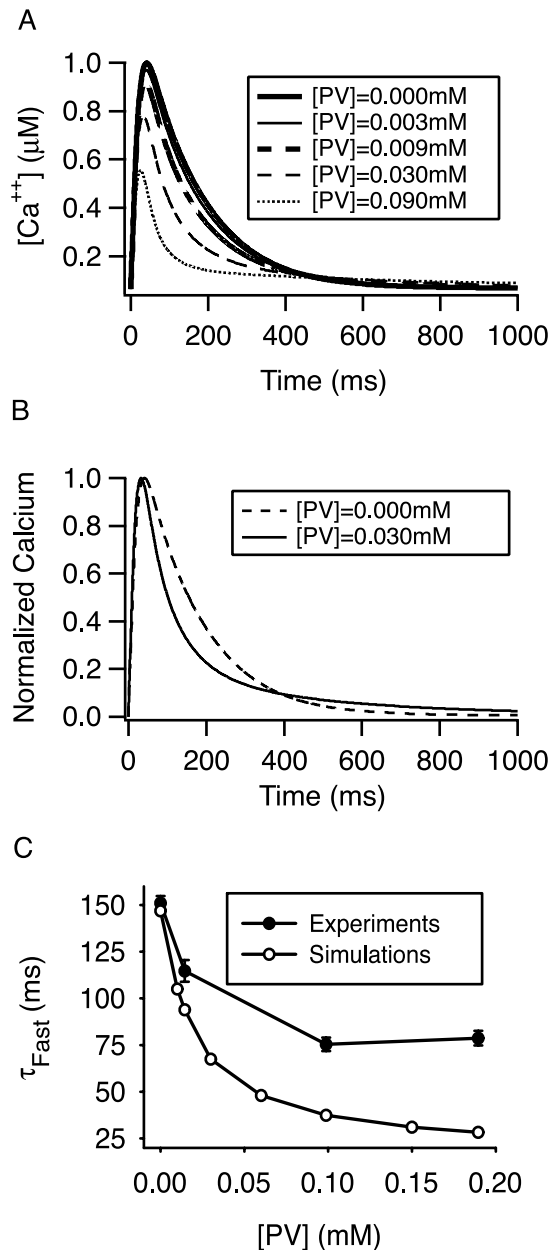
FIGURE 8 Simulation of the buffering effects of PV on the calcium transients (fixed calcium release model). (*A*) Effects of [PV] on the time course of the calcium transient; (*B*) Normalized response from two of the traces ([PV] = 0.000 mM and 0.030 mM) displayed in *A*; (*C*) Comparison between experimental and theoretical dose-response relationship for the fast time constant of the decay. For [PV] = 0.0 mM, the single time constant was used.

effect of PV binding on the calcium transients to extract useful information. The fixed calcium release model represents a simplified version of the myocyte environment. Indeed, as mentioned in Methods, the model includes calcium release and uptake compartments as well as buffering by calmodulin, troponin, and PV. Fig. 8 *A* shows the effect of PV concentration on the time course of the calcium

transient. The frequency of stimulus was chosen to be 0.2 Hz, and 20 cycles were allowed to reach a dynamic buffering steady state. For [PV] < 0.003 mM, PV has very little effect on the calcium transient. For 0.003 mM ≤ [PV] < 0.03 mM, there is an increase in the rate of decay with little or no effects on the rising phase of the transient. As PV increases above 0.03 mM, although the calcium transient decays even faster, its amplitude is also reduced. To make comparisons with the experimental results presented earlier, the resulting calcium transient for the PV-free and [PV] = 0.03 mM simulations were normalized and are presented in Fig. 8 *B*. Single- and double-exponential fits were performed on the decay phase of the PV-free and [PV] = 0.03 mM, respectively. By model construction, a decay time constant ($\tau$) of 148.1 ms was obtained for the control transient (PV free), which is comparable to the result obtained experimentally (Table 1: $\tau$ = 151.0 ± 3.8ms). Using the same stimulus, but increasing [PV] to 0.03 mM, produced results very similar to those obtained on day 3 (model versus experimental results in Table 1: $\tau_{FAST}$ = 67.5 vs. 75.4 ± 3.6ms, $\tau_{SLOW}$ = 401.5 vs. 898 ± 72ms; relative amplitude of the slow component: 14.9 vs. 11.9 ± 1.1%). However, Western blot results indicate an estimated PV concentration of 0.099 ± 0.012 mM, which is somewhat higher than the 0.03 mM indicated by the model (Fig. 8 *C*). Among the possible reasons for this discrepancy in the level of [PV] required to reach similar response, is the degree of uncertainty on the on and off rates in Eqs. 1 and 2. As mentioned earlier, these values were extrapolated from experimental results obtained in different species under different temperature conditions. By simply dividing $k^+_{pvca}$ by 1.8 and $k^-_{pvmg}$ by 3.3 and increasing [PV] to 0.09 mM, a very similar curve to the [PV] = 0.03 mM curve presented in Fig. 8 *B* was obtained (simulation results not shown because the two curves almost overlap). Other issues regarding this apparent mismatch will be presented in the Discussion.

The effects of altered stimulation frequency on the calcium transient were also investigated using simulations. The fixed calcium transient model was used to study the effect of changes in *Pvca* during a single contraction. Fig. 9 *A* shows the fixed calcium transient used as stimulus (4.0 Hz shown). A minimum of 50 s (simulation time) was allowed for the *Pvca* and *Pvmg* to reach their dynamic steady states. After reaching the dynamic steady state, the amplitude of *Pvca* was plotted against time (Fig. 9 *B*). As the frequency of stimulation increased, the average level of PV occupation by calcium increased. However, as the frequency increases the variation in *Pvca* (Δ*Pvca*) decreases (Fig. 9 *C*). As mentioned earlier, for a given PV concentration, it is Δ*Pvca*, not the *Pvca* absolute value, that dictates how much calcium can be buffered during a single beat. Therefore, for a given PV concentration, calcium buffering capacity decreases as stimulation frequency is increased.
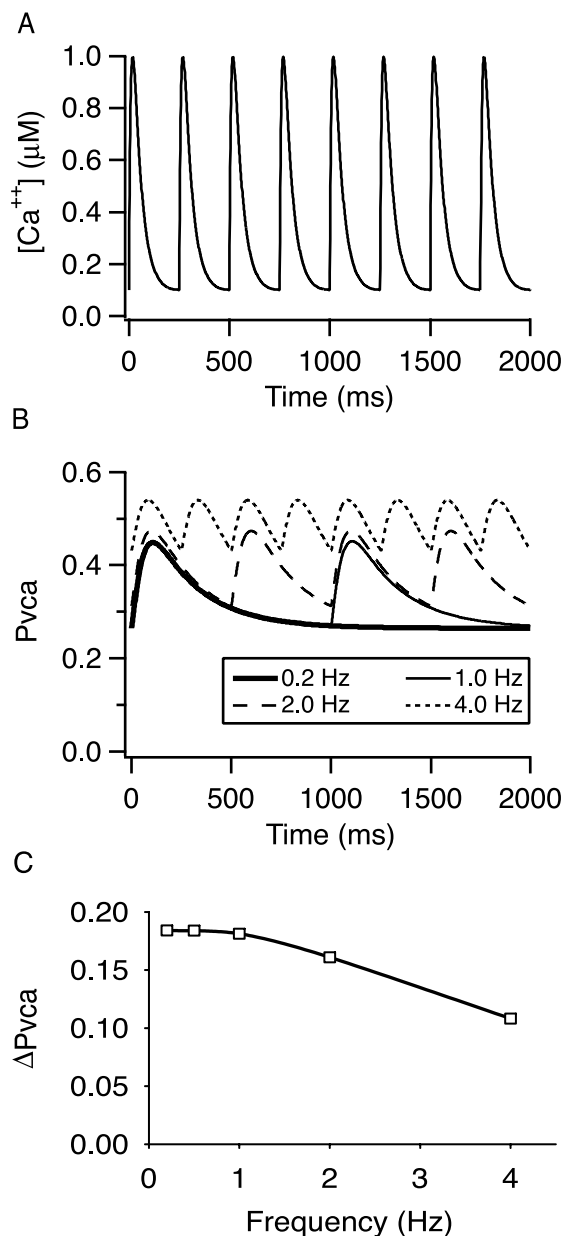
FIGURE 9 Simulation of PV fractional binding to calcium as function of stimulus frequency (fixed calcium transient model). (*A*) Fixed shaped calcium transient used as control variable (example shown is at $f = 4.0$ Hz); (*B*) Time course of the fractional binding of calcium to PV (*Pvca*) when submitted to the fixed calcium transient at different frequencies (traces shown under dynamic steady-state conditions); (*C*) Summary of the amplitude of $\Delta Pvca$ (variation in *Pvca*) for the different frequencies modeled.

## DISCUSSION

An important contribution of this study is that it establishes for the first time the PV dose-response relationship in adult cardiac myocytes. A combined approach of experimental work and mathematical modeling was used to investigate the quantitative effects of PV not only on relaxation but also

on contractile cellular properties. For the experimental work, gene transfer technology was applied to isolated cardiac myocytes from adult rats. The level of PV expression was varied by examining cardiac myocytes at different time points after gene transfer, from initial detection (day 2) to apparent saturation (day 4). This strategy is made possible by the high efficiency (>95%) and synchronization of PV gene transfer to cardiac myocytes. From these attributes of gene transfer, we conclude that global quantitative analysis of PV expression is highly correlated to alterations at the level of the single myocyte. We measured calcium transient dynamics in single cardiac myocytes using the fluorescent indicator fura-2 and unloaded shortening contraction properties using a laser diffraction system. Different mathematical models, each incorporating equations of the law of mass action for PV binding to calcium and magnesium, were used to gain mechanistic insights into PV function in cardiac myocytes.

## Determining the optimal range for PV functional effects

To establish the threshold effects of PV it was first ascertained that for the non-transduced myocytes (controls), there were no significant changes on any of the properties of the shortening contraction from day 1 to 4 in primary culture. This provided a unique and stable system to modify PV expression by gene transfer. Second, using a virus containing the *Lac-Z* gene neither the calcium kinetics nor contractile function were affected, indicating no specific or nonspecific effects of gene transfer on these parameters. In this experimental setting, results demonstrated a specific PV expression range where the $t_{S-1/2R}$ was decreased without having any significant effects on contractile amplitude. This occurred on day 2.5 after gene transfer (Fig. 5). On day 2.5, the average estimated concentration of PV, as detected using Western Blots, was 0.048 mM. At earlier time points, and correspondingly lower levels of PV, there were no significant alterations in relaxation in cardiac myocytes. At later time points, where PV concentration was increased (~0.1 mM), relaxation rates further accelerated (Fig. 5). However, at these higher concentrations of PV there was a significant reduction in contractile amplitude. These results suggest that the optimal range of PV expression, where contraction is hastened without attenuation in amplitude, is between ~0.01 and ~0.1 mM.

To gain mechanistic insights into the effects of PV on the calcium transient, we constructed a mathematical model in which PV buffering equations were mixed with a calcium source, a calcium sink, and other cystolic calcium buffers (troponin and calmodulin). This model had a fixed release equation that was chosen to give a typical calcium transient in the absence of PV. Using this constant calcium release model, there were three different effects on the calcium transients. At low PV concentrations ([PV] ≤ 0.003 mM),

little or no effect was seen. At intermediate levels (0.003 mM < [PV] < 0.03 mM), there was an acceleration in the calcium transient decay rate with little or no attenuation in the amplitude of the transient. At higher concentrations ([PV] $\geq$ 0.03 mM), although the calcium transient had a much faster decay, the amplitude started to decrease as the PV level increased. This would lead to a theoretical optimal range of PV concentration from 0.003 to 0.03 mM for which the decay rate is quicker and amplitude not significantly altered. This range is somewhat lower than the experimental range mentioned above. Possible reasons for this discrepancy will be discussed below.

## PV causes a plateau in the SL shortening-frequency relationship

In agreement with recent studies (Lim et al., 2000), control cardiac myocytes exhibited a biphasic SL shortening-frequency relationship. There was a negative staircase from 0.2 to 1.0 Hz, whereas the range from 2.0 to 4.0 Hz exhibited a positive staircase. In PV-expressing myocytes the SL shortening-frequency relationship was mostly flat. Similar observations were made when the $t_{S-1/2R}$ was plotted as a function of the frequency. Upon examination of the raw non-normalized data, it was evident that PV-expressing myocytes have a faster relaxation and a lower amplitude when compared with the control myocytes at 0.2 Hz. However, when the frequency increases, these functional differences tended to decrease. Thus, the PV-expressing myocytes behaved more similar to control myocytes in terms of relaxation kinetics at the highest stimulation frequency.

In an attempt to understand the mechanism of this response, mathematical modeling was used. The effect of stimulation frequency on the fractional binding of calcium to PV was investigated using the fixed calcium transient model. This model was chosen to eliminate the variations in the calcium transient due to PV buffering, thereby allowing a fair comparison between simulation results at each frequency. As shown in Fig. 9, $\Delta Pvca$ (variation in fractional binding of PV to calcium) decreases as the stimulation frequency increases. This is due to the fact that the binding and unbinding reactions from PV do not have time to come to completion when the inter-beat duration is reduced. This reduction in $\Delta Pvca$ at high frequency, which would result in an effectively lower amount of calcium buffered during the decaying phase of the transient, could explain, at least in part, why the PV myocytes tend to behave more similarly to control myocytes. An interesting outcome of this analysis is that PV would be predicted to have little effect on relaxation function in transgenic mouse hearts in vivo because of the high heart rates in mice ($\sim$600 beats per minute). In contrast, it is expected that for equivalent PV concentrations, the impact on relaxation would be greater in larger mammals where the heartbeat is slower ($\sim$60–100 beats per minute).

## Presence of PV changes the calcium transient decay fit from single- to double-exponential relationship

For all control myocytes and *Lac-Z*-transduced myocytes, a single-exponential function was sufficient to accurately fit the calcium transient decay data. However, for a large portion of the PV myocytes studied ($\sim$80%), using a double-exponential function dramatically increased the quality of the fit. The same phenomenon has been seen experimentally in mouse skeletal muscle endogenously expressing PV (Westerblad and Allen, 1994) or in rat cardiac myocytes loaded with NP-EGTA (a slow calcium buffer) that also produced a fast and a slow decay phase (Diaz et al., 2001). In the present study, the PV-expressing myocytes had a fast decay component ($\sim$87% of the amplitude) with a time constant decreasing as the level of PV increases. The slow component had a time constant of much longer duration ($\sim$900 ms for all days combined), which seemed to be less dependent on absolute PV concentration. Using normalized calcium transient simulation results, a similar behavior to those obtained experimentally was observed. In particular, we examined two simulated PV concentrations. At [PV] = 0.0 mM (PV free), the model gave very similar time constants to the ones obtained in control myocytes experimentally. Next, we increased PV concentration (the only free parameter) until we had a behavior similar to day 3 experimental data. Interestingly, the model also exhibited a clear double-exponential decay curve (Fig. 8 *B*). At [PV] = 0.03 mM, the fast component contribution and fast time constant were also very similar to those obtained experimentally (see Results). The slow time constant, even though smaller, was of the same order of magnitude. The mechanism underlying the change from single-exponential fit to double-exponential fit in the presence of PV could be explained as follows. As described in the Introduction, delayed calcium buffering by PV is responsible for the strong buffering in the early decay phase of the transient. However, when the calcium level starts to return to its resting value the extra calcium absorbed by PV during the rise and the early decay of the calcium transient is now released in the late part of the cycle. This process is also a slow one and is primarily dictated by the calcium off rate constant from PV (modifying $k_{pvca}^-$ in the fixed calcium release model had a major influence on the amplitude and kinetics of the slow component of the calcium transient, data not shown). Therefore, in the late part of the cycle, PV acts as a slow source of calcium release (not present in control myocytes). This source effect is mostly responsible for the slower decay toward the end of the cycle, explaining the presence of a second (slow) exponential component.

## Limitations of the study

There are some limitations to this study. First, as mentioned throughout the text, the on and off rates for PV-related reactions were obtained under different conditions and thus impact the quantitative simulation results. However, the qualitative behavior of the models was certainly sufficient to explain several of the phenomenon seen experimentally, such as the effects of PV on calcium transient amplitude and decay rate, the decreased effects of PV with increasing stimulus frequency, and the transition in the calcium transient decay from single to double exponential when PV was present.

Second, there was a discrepancy between the experimental and simulation determined optimal range of PV. This could be due to the uncertainties in the quantitative results of the models, but it should be also noted that the experimentally determined PV concentration is only an estimate. Indeed, the estimated level of PV expression was normalized to actin in both the reference (SVL) and the PV-transduced myocytes. Because there are more myofilament proteins in fast skeletal muscles than in cardiac myocytes (Bers, 2001), it is possible that the experimental PV concentration might have overestimated PV in the transduced cardiac myocytes.

Finally, it should be pointed out that this study was performed in rat adult cardiac myocytes in primary culture under unloaded conditions. The optimal range of PV might be different in cardiac myocytes from different species, under loaded conditions, or in the intact heart.

## Implications

Diastolic dysfunction is characterized by a slow relaxation and is found in 40% of the patients with heart failure (Lorell, 1991). In this and other studies (Wahr et al., 1999), we have shown an increase in calcium transient decay rate in isolated adult cardiac myocytes in the presence of PV. More specifically, in the present study, we demonstrated experimentally and theoretically that there exists a critical PV concentration range for which the relaxation rate is increased without attenuation in the contractile amplitude. At PV levels below this critical range in PV concentration there were no effects on contractile properties. Above this critical range, the relaxation was further accelerated, but there was also a significant reduction in contractile amplitude. We recently demonstrated the effects of PV gene transfer on contractile relaxation in vivo (Szatkowski et al., 2001). The results showed not only a faster relaxation time when compared with normal control rat hearts but also increased contractile properties (higher $dP/dt$). The basis for this latter effect is unknown but likely involves the complexity of organ level function in intact animals, factors that are missing in the isolated cardiac myocytes used in the present study.

In summary, the present study demonstrates a critical PV concentration range in isolated cardiac myocytes for which the systolic parameters of the contraction remained unaffected while diastolic relaxation was accelerated. This range was determined experimentally to be ~0.01–0.10 mM and theoretically to be 0.003–0.030 mM. Establishing the expression threshold for PV exerting physiological effects has implications for the use of PV as a cardiac relaxing factor in normal and pathological states in vivo.

## REFERENCES

Bers, D. M. 2001. Excitation-Contraction Coupling and Cardiac Contractile Force. Kluwer Academic Publishers, Dordrecht, The Netherlands.

Diaz, M. E., A. W. Trafford, and D. A. Eisner. 2001. The effects of exogenous calcium buffers on the systolic calcium transient in rat ventricular myocytes. *Biophys. J.* 80:1915–1925.

Eberhard, M. and P. Erne. 1994. Calcium and magnesium binding to rat parvalbumin. *Eur. J. Biochem.* 222:21–26.

Feher, J. J., T. D. Waybright, and M. L. Fine. 1998. Comparison of sarcoplasmic reticulum capabilities in toadfish (*Opsanus tau*) sonic muscle and rat fast twitch muscle. *J. Muscle Res. Cell Motil.* 19: 661–674.

Gerald, C. F., and P. O. Weathley. 1985. Applied Numerical Analysis. Addison-Wesley, New York.

Godt, R. E. and D. W. Maughan. 1988. On the composition of the cytosol of relaxed skeletal muscle of the frog. *Am. J. Physiol.* 254:C591–C604.

Green, H. J., G. A. Klug, H. Reichmann, U. Seedorf, W. Wiehrer, and D. Pette. 1984. Exercise-induced fibre type transitions with regard to myosin, parvalbumin, and sarcoplasmic reticulum in muscles of the rat. *Pflugers Arch.* 400:432–438.

Hattori, Y., J. Toyama, and I. Kodama. 1991. Cytosolic calcium staircase in ventricular myocytes isolated from guinea pigs and rats. *Cardiovasc. Res.* 25:622–629.

Heizmann, C. W., M. W. Berchtold, and A. M. Rowlerson. 1982. Correlation of parvalbumin concentration with relaxation speed in mammalian muscles. *Proc. Natl. Acad. Sci. U.S.A.* 79:7243–7247.

Hou, T. T., J. D. Johnson, and J. A. Rall. 1991. Parvalbumin content and $Ca^{2+}$ and $Mg^{2+}$ dissociation rates correlated with changes in relaxation rate of frog muscle fibres. *J. Physiol.* 441:285–304.

Hou, T. T., J. D. Johnson, and J. A. Rall. 1992. Effect of temperature on relaxation rate and $Ca^{2+}$, $Mg^{2+}$ dissociation rates from parvalbumin of frog muscle fibres. *J. Physiol.* 449:399–410.

Lim, C. C., C. S. Apstein, W. S. Colucci, and R. Liao. 2000. Impaired cell shortening and relengthening with increased pacing frequency are intrinsic to the senescent mouse cardiomyocyte. *J. Mol. Cell Cardiol.* 32:2075–2082.

Lorell, B. H. 1991. Significance of diastolic dysfunction of the heart. *Annu. Rev. Med.* 42:411–436.

Morgan, J. P. 1991. Abnormal intracellular modulation of calcium as a major cause of cardiac contractile dysfunction. *N. Engl. J. Med.* 325: 625–632.

Pauls, T. L., J. A. Cox, and M. W. Berchtold. 1996. The Ca2+(-)binding proteins parvalbumin and oncomodulin and their genes: new structural and functional findings. *Biochim. Biophys. Acta.* 1306:39–54.

Rall, J. A. 1996. Role of parvalbumin in skeletal muscle relaxation. *News Physiol. Sci.* 11:249–255.

Robertson, S. P., J. D. Johnson, and J. D. Potter. 1981. The time-course of $Ca^{2+}$ exchange with calmodulin, troponin, parvalbumin, and myosin in response to transient increases in $Ca^{2+}$. *Biophys. J.* 34:559–569.

Rome, L. C. and A. A. Klimov. 2000. Superfast contractions without superfast energetics: ATP usage by SR-$Ca^{2+}$ pumps and crossbridges in toadfish swimbladder muscle. *J. Physiol.* 526:279–286.

Rome, L. C., C. Cook, D. A. Syme, M. A. Connaughton, M. Ashley-Ross, A. Klimov, B. Tikunov, and Y. E. Goldman. 1999. Trading force for speed: why superfast crossbridge kinetics leads to superlow forces. *Proc. Natl. Acad. Sci. U.S.A.* 96:5826–5831.

Shannon, T. R., K. S. Ginsburg, and D. M. Bers. 2000. Reverse mode of the sarcoplasmic reticulum calcium pump and load-dependent cytosolic calcium decline in voltage-clamped cardiac ventricular myocytes. *Biophys. J.* 78:322–333.

Spirito, P., P. Bellone, K. M. Harris, P. Bernabo, P. Bruzzi, and B. J. Maron. 2000. Magnitude of left ventricular hypertrophy and risk of sudden death in hypertrophic cardiomyopathy. *N. Engl. J. Med.* 342:1778–1785.

Stemmer, P. and T. Akera. 1986. Concealed positive force-frequency relationships in rat and mouse cardiac muscle revealed by ryanodine. *Am. J. Physiol.* 251:H1106–H1110.

Szatkowski, M. L., M. V. Westfall, C. A. Gomez, P. A. Wahr, D. E. Michele, C. DelloRusso, I. I. Turner, K. E. Hong, F. P. Albayya, and J. M. Metzger. 2001. In vivo acceleration of heart relaxation performance by parvalbumin gene delivery. *J. Clin. Invest* 107:191–198.

Wahr, P. A., D. E. Michele, and J. M. Metzger. 1999. Parvalbumin gene transfer corrects diastolic dysfunction in diseased cardiac myocytes. *Proc. Natl. Acad. Sci. U.S.A.* 96:11982–11985.

Westerblad, H. and D. G. Allen. 1994. Relaxation, $[Ca^{2+}]_i$ and $[Mg^{2+}]i$ during prolonged tetanic stimulation of intact, single fibres from mouse skeletal muscle. *J. Physiol.* 48:31–43.

Westfall, M. V., E. M. Rust, F. Albayya, and J. M. Metzger. 1997. Adenovirus-mediated myofilament gene transfer into adult cardiac myocytes. *Methods Cell Biol.* 52:307–322.

Winslow, R. L., J. Rice, S. Jafri, E. Marban, and B. O'Rourke. 1999. Mechanisms of altered excitation-contraction coupling in canine tachycardia-induced heart failure. II. model studies. *Circ. Res.* 84:571–586.